agriculture

MDPI

Article

Study on the Performance of Filters Under Biogas Slurry Drip Irrigation Systems

Shuaijie Wang [1,2,3,†], Haitao Wang [3,†], Xuefeng Qiu [3], Jiandong Wang [2,3], Shuji Wang [1,*], Hang Wang [2,3] and Tao Shen [4,*]

[1] School of Water Conservancy and Hydroelectric Power, Hebei University of Engineering, Handan 056038, China; w15518578955@163.com
[2] Western Agricultural Research Center, Chinese Academy of Agricultural Sciences, Changji 831100, China; wangjiandong@caas.cn (J.W.); 82101221175@caas.cn (H.W.)
[3] Institute of Environment and Sustainable Development in Agriculture, Chinese Academy of Agricultural Sciences, Beijing 100081, China; wanghaitao@caas.cn (H.W.); qiuxuefeng@caas.cn (X.Q.)
[4] Anhui & Huaihe River Institute of Hydraulic Research, Bengbu 233000, China
* Correspondence: wangshuji@hebeu.edu.cn (S.W.); shentao97@163.com (T.S.)
† These authors contributed equally to this work.

Abstract: Filters are essential components for maintaining the stability of drip irrigation systems, effectively reducing the risk of clogging. However, when applied to slurry drip irrigation systems, the complexity of slurry water quality makes it unclear how different filter types and their combinations affect the hydraulic performance of the system. This study provides a comprehensive performance evaluation of two common filter types and their combinations, considering various flow rates and biogas slurry-to-water ratios under drip irrigation conditions. The results revealed the following key findings: (1) In the application of biogas slurry drip irrigation, an increase in the concentration or flow rate of the slurry significantly affects the hydraulic performance of the filter, increasing the risk of clogging and shortening the operational lifespan. Notably, the impact of changes in slurry concentration on the hydraulic performance of the filter is much greater than that of the flow rate. Compared to mesh filters, disk filters offer better hydraulic performance, with the contaminant capacity of disk filters being approximately three times that of mesh filters. (2) In biogas slurry drip irrigation, the filter combination generally outperforms single filters in terms of hydraulic performance and contaminant removal capacity. Due to the unique nature of the water source in biogas slurry, a selection process for filter combinations was conducted. It was found that when a disk filter is used as the pre-filter and a mesh filter as the post-filter, the overall rate of head loss change is the smallest, and the clogging uniformity is the least. (3) In the entropy weight-TOPSIS comprehensive evaluation, the filter's operating time and contaminant capacity are key factors affecting its overall performance. From the perspective of improving the operational stability of the biogas slurry drip irrigation system, it is recommended to use a disk filter + mesh filter combination. This study conducts practical measurements on the hydraulic performance, contaminant removal capacity, filtration accuracy, and other indicators of commonly used mesh and disk filters, aiming to provide useful references for the practical application of biogas slurry drip irrigation filters.

Keywords: filter; head loss; pollutant carrying capacity; biogas slurry; comprehensive evaluation

check for updates

Academic Editors: Andrea Pezzuolo, Francesca Valenti and Monica Concetta Maria Parlato

Received: 16 November 2024
Revised: 23 December 2024
Accepted: 24 December 2024
Published: 26 December 2024

Citation: Wang, S.; Wang, H.; Qiu, X.; Wang, J.; Wang, S.; Wang, H.; Shen, T. Study on the Performance of Filters Under Biogas Slurry Drip Irrigation Systems. *Agriculture* **2025**, *15*, 30. https://doi.org/10.3390/agriculture15010030

Copyright: © 2024 by the authors. Licensee MDPI, Basel, Switzerland. This article is an open access article distributed under the terms and conditions of the Creative Commons Attribution (CC BY) license (https://creativecommons.org/licenses/by/4.0/).

1. Introduction

As a nutrient-rich liquid fertilizer, biogas slurry has garnered increasing attention in the agricultural sector in recent years [1]. Its rational utilization is seen as a key solution to the growing problem of excess wastewater and shortage of water resources [2,3]. Biogas slurry is produced during the anaerobic biodegradation of organic waste, and its production scale continues to grow alongside the intensive, large-scale development of livestock and poultry farming [4]. If discharged directly, biogas slurry can cause significant environmental pollution [5]. Although biogas slurry can be treated and purified into regenerated water through complex sewage treatment processes to meet discharge standards, this approach is energy-intensive and costly and leads to a loss of valuable nutrient resources [6]. Therefore, there is an urgent need to explore more economical, environmentally friendly, and efficient methods for treating biogas slurry. In this context, the crop breeding cycle model has been proposed, advocating for the direct reuse of biogas slurry as an organic fertilizer for farmland irrigation. This approach not only facilitates the resource utilization of wastewater but also helps mitigate global water scarcity.

Drip irrigation, known for its labor-saving, efficient, and controllable nature, is considered the most promising technology and engineering solution for the efficient utilization of biogas slurry in agricultural fields [7]. However, the use of biogas slurry in drip irrigation systems has highlighted several challenges, particularly due to its complex composition. Biogas slurry contains a large amount of suspended particles, organic matter, microorganisms, and other impurities. When these contaminants enter the farmland through the drip irrigation system, they can easily clog the emitters and filters, disrupting the system's normal operation and the uniformity of water and fertilizer distribution [8,9]. This, in turn, may negatively impact crop yield and quality. Therefore, developing or identifying efficient and reliable filter systems for biogas slurry drip irrigation is crucial for ensuring the long-term performance of these systems. In recent years, extensive research has been conducted both domestically and internationally on optimizing wastewater filtration technologies. Current studies mainly focus on testing the hydraulic performance of filters and simulating the internal water flow characteristics. In efforts to improve filter anti-clogging performance, some researchers have suggested that ultrasonic irradiation during wastewater filtration can effectively reduce filter fouling [10]. Others have found that using combination filters can enhance filtration quality, reduce heavy metal contamination, and improve filtration efficiency [11,12]. Additionally, several studies have simulated the hydraulic behavior of filters, including water flow, pressure drop, velocity distribution, and the impact of porous media on water movement within filters under drip irrigation conditions. Based on these simulations, optimization designs for filters have been proposed [13]. Furthermore, some researchers have recommended specific filter types for different water quality conditions [14,15]. However, for biogas slurry drip irrigation systems, the impact of the unique and complex composition of biogas slurry on the performance of existing filters remains unclear. This is especially true for field applications, where the slurry needs to be diluted and rebalanced with clean water. There is a lack of relevant research on the operational performance characteristics and influencing factors of different filter types under various biogas slurry dilution ratios and flow conditions, which still needs to be explored in greater depth. (1) To clarify the influence of system flow rate, slurry concentration, and filter type on the hydraulic and pollutant-carrying performance of filters in biogas slurry drip irrigation systems. (2) To identify the key factors affecting the overall performance of filters in biogas slurry drip irrigation systems. (3) To select appropriate filter types and combinations for optimal performance in biogas slurry drip irrigation systems.

2. Materials and Methods

2.1. Experimental Apparatus

The experiment was conducted in 2022 at the Experimental Station of the Academy of Agricultural Sciences in Shouyang County, Shanxi Province. The experimental device consists of water pump, water bucket, head gauge, filter, valve, main pipe, branch pipe, and other equipment. The experimental layout is shown in Figure 1. There is a return valve downstream of the check valve (Xiamen Xieyu Plastic Co., Ltd., Xiamen, China) at the outlet of the water pump (rated head: 25 m, 1.5ZDK-1800, Jiangsu New World Pump Industry Co., Ltd., Jingjiang, China), and the filter(Beijing Yijia Ideal Water Purification Equipment Co., Ltd., Beijing China) is located between the return valve and the main valve. Four types of filters, including screen mesh and disk filters (80 mesh and 120 mesh), are selected. Pressure regulating valves are installed at the inlet of each branch pipe to adjust the operating pressure of the drip irrigation system. A pressure gauge is installed at the end of the filter to ensure that the pressure at the end of the filter is stable at 0.1 MPa (the working pressure of the drip irrigation system's field pipeline network). The test device is equipped with a return valve to prevent the water pump from idling. An electromagnetic flow meter is installed in front of the filter to measure changes in the inlet flow rate of the filter. Install two pressure gauges (with an accuracy level of 0.25 and a range of 0~0.25 MPa, Hongqi Instrument Co., Ltd., Wenzhou, China) in the inlet and outlet sections of the filter to facilitate the observation of local head loss in the combined filter.

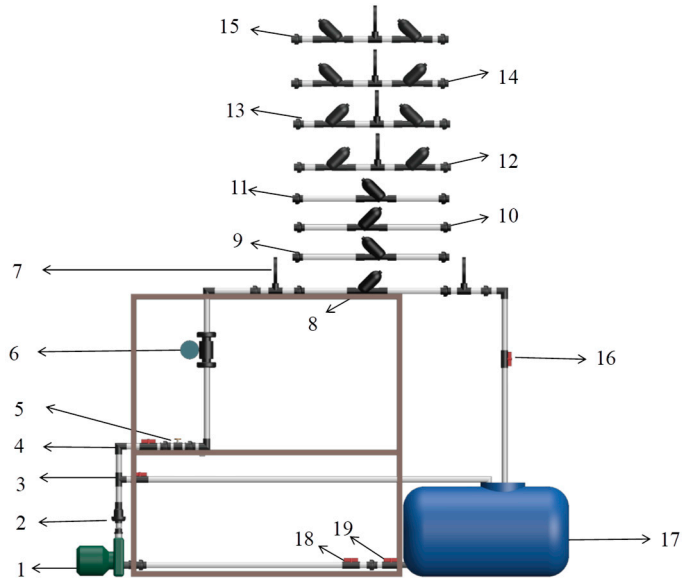


Figure 1. Filter hydraulic performance testing platform. 1. Water pump. 2. Check valve. 3. Reflux valve. 4. Flow regulating ball valve. 5. Flow regulating diaphragm valve. 6. Electromagnetic flow meter. 7. Pressure gauge. 8. 80 screen mesh filter. 9. 80 disk filter. 10. 120 screen mesh filter. 11. 120 disk filter. 12. S80 + S120. 13. S80 + D120. 14. D80 + S120. 15. D80 + D120. 16. Tail pressure regulating valve. 17. Water bucket. 18. Water pump inlet valve. 19. Bucket outlet valve.

2.2. Experimental Design

2.2.1. Hydraulic Performance Test of Drip Irrigation Filter for Clear Water

When passing through clean water, the filter will not clog, but it will still generate a certain pressure loss and maintain this pressure loss level after stabilization. Before conducting hydraulic performance tests on biogas slurry drip irrigation filters, it is helpful to clarify the changes in pressure loss of different filters and their combinations with flow rate under clear water conditions, which helps to deeply analyze the impact of biogas slurry on filter performance. Two types of filters (screen mesh and disk) and two

filtering accuracies (80 mesh and 120 mesh) were selected for hydraulic performance testing separately and in combination. When conducting the combination test, 80 mesh was selected as the primary filter and 120 mesh as the secondary filter. The testing plan is shown in Table 1. According to the flow rate requirements of the filter, test the pressure loss at inlet flow rates of 1.5 m^3/h, 2 m^3/h, 2.5 m^3/h, 3 m^3/h, and 3.5 m^3/h. Before measurement, allow the system to run stably for 5 min under the corresponding flow conditions, and measure the local head loss of the filter at the selected flow rate (the difference in pressure between the inlet and outlet of the filter).

Table 1. Hydraulic performance testing scheme for filters.

Classification Number	Filter Type
S1	80 mesh screen mesh
S2	80 mesh disk
S3	120 mesh screen mesh
S4	120 mesh disk
S5	80 mesh screen mesh + 120 mesh screen mesh
S6	80 mesh screen mesh + 120 mesh disk
S7	80 mesh disk + 120 mesh screen mesh
S8	80 mesh disk + 120 mesh disk

2.2.2. Hydraulic Performance Testing of Biogas Slurry Drip Irrigation Filters

After completing the hydraulic performance of the clear water drip irrigation filter, the hydraulic performance test of the biogas slurry drip irrigation filter adopts a two-factor and three-level experimental design, with two factors being the inlet flow rate and the biogas slurry concentration (volume ratio of biogas slurry to clear water). Among them, the inlet flow rate is set at three levels: 1.5 m^3/h, 2.5 m^3/h, and 3.5 m^3/h. According to Wang et al. [3,16], the method of combining biogas slurry with water was used, and the biogas slurry concentration (volume ratio of biogas slurry to clean water) is set at three levels: 1:9, 1:14, and 1:19.

When exploring the influence of inlet flow rate on the hydraulic and pollutant absorption performance of the filter, the biogas slurry concentration was kept at 1:14, and the inlet flow rates were set at 1.5 m^3/h, 2.5 m^3/h, and 3.5 m^3/h. When exploring the effect of biogas slurry concentration on the hydraulic and pollutant absorption performance of filters, the inlet flow rate was maintained at 2.5 m^3/h, and the biogas slurry concentrations were set at 1:9, 1:14, and 1:19. The clean water used in the experiment is local tap water. The original biogas slurry for the experiment was selected from pretreated biogas slurry, and different concentration levels of biogas slurry were set according to the method of Wang et al. [3] for mixing biogas slurry with water. The parameters are shown in Table 2. During the experiment, record the pressure difference before and after the filter at regular intervals. When the head loss exceeds 5 meters, it is considered severe blockage [17]. Stop the experiment, and record the running time T. After each test is completed, remove the filter for flushing, and ensure the conductivity Ec inside the drum remains consistent before each test starts by adding appropriate water or biogas slurry. Repeat the test three times for each operating condition.

Table 2. Bottom value of biogas slurry.

	Original Biogas Slurry	Test Biogas Slurry (1:9)	Test Biogas Slurry (1:14)	Test Biogas Slurry (1:19)
EC (μs/cm)	18,960	2030	1320	980
SS (mg/L)	2560	274	190	115

2.3. Test Indicators

2.3.1. Filter Head Loss

Under specific conditions, the relationship between head loss and flow rate can be simplified into a mathematical expression [18]. When water flows through the filter, determine the relationship between head loss and flow rate based on measured values. Therefore, we can use Formula (1) to represent the relationship between head loss h and flow rate q, where head loss can be converted from measured pressure loss values, and 1 MPa pressure loss is approximately equal to 100 m head loss.

$$h = kq^{\alpha} \quad (1)$$

where h indicates head loss, m; q indicates the flow rate inside the pipeline, m^3/h; k are constants related to the structure of filter cartridges and fluid properties; and α is the exponential relationship between the flow rate inside the filter and the head loss.

2.3.2. Filter Operating Time

The time from the start of filter operation until severe system blockage occurs is defined as the filter operating time.

2.3.3. Increase Rate of Head Loss

The ratio of head loss to duration at different stages is defined as the rate of increase in head loss [19], which can be expressed by Formula (2).

$$\delta_i = \frac{h_{i+1} - h_i}{t_i} \quad (2)$$

where δ_i increases the rate of head loss for stage i,m/min; h_{i+1} is the head loss at the end of stage i,m; h_i is the initial head loss for stage i,m; and t_i is the corresponding running time for each stage.

2.3.4. Uniformity of Blockage

Some scholars divide the operation stage of the filter into a stable operation period (t_1) and a blockage operation period (t_2) and define the ratio of the growth rate of head loss in the two stages as the blockage uniformity index [19]. This article divides the operation stage of the filter into a stable operation period (t_1) and a blocking operation period (t_2) based on the rate of increase in filter head loss. The stable operation stage refers to the rate of change in filter head loss remaining relatively stable for a period of time, while the blocking operation stage refers to the rate of change in filter head loss suddenly increasing rapidly for a period of time. The rate of change in head loss at the junction of the two stages is greater than or equal to 10%. The ratio of the rate of increase in head loss in the first stage to the rate of increase in head loss in the second stage is defined as the blockage uniformity, which can be expressed by Formula (3).

$$\eta = \frac{\delta_2}{\delta_1} \quad (3)$$

2.3.5. Filter Capacity

The measurement of the pollutant holding capacity of each filter combination adopts the weighing method [20]. By measuring the retention capacity of each group of stainless steel filter elements and drying them at 105 °C for 24 h to a constant weight, using an electronic scale with an accuracy of 0.001 g, the sum of the dry weight (DW) of the filter element and its pollutant holding capacity is obtained. The difference between the DW of

the filter element and its pollutant holding capacity is the DW of the combined pollutant holding capacity of the filter element. Calculate the DW of the filter cartridge for different treatments using Formula (4).

$$DW = S_2 - S_1 \tag{4}$$

where S_1 indicates the DW of the filter element, mg; S_2 indicates the total DW of the filter element and its pollutant holding capacity, mg; and DW indicates the amount of dirt carried by the filter element, mg.

2.4. Comprehensive Evaluation of Performance of TOPSIS Filter Based on Entropy Weight

The entropy weight TOPSIS method, combined with weighted indicators, effectively captures the differences between various schemes [21,22]. Based on experimental data, this method is used to evaluate the impact of different filter indicators on overall performance. The evaluation indicators include running time (T), filter element mesh size (M), and filter capacity (DW), all of which are positive indicators, with M being closely related to filtration accuracy. Blockage uniformity (η) and initial head loss (h_j) are considered negative indicators. To account for the differences between these indicators, the entropy weight method is applied to assign weights to each evaluation factor and rank the influence of each on the filter's overall performance. The specific process is as follows.

(1) First, establish a data matrix and standardize the head loss index. Let X_{mn} represent the evaluation index for each processing set in the evaluation. The indicators for each processing set are combined to form a data matrix X = (X_{mn}) M × N ($1 \leq m \leq M$; $1 \leq n \leq N$). To eliminate the influence of dimensionality, the data matrix is standardized to create the standardized matrix Z = (Z_{mn}) M × N ($1 \leq m \leq M$; $1 \leq n \leq N$). Both positive and negative indicators are processed in the same direction to ensure data comparability. The raw data is standardized according to the formulas shown in Equations (5) and (6).

$$Z_{mn} = \frac{X_{mn} - X_{min}}{X_{max} - X_{min}} \tag{5}$$

$$Z'_{mn} = \frac{X_{max} - X_{mn}}{X_{max} - X_{min}} \tag{6}$$

where Z_{mn} standardizes the matrix for positive indicators and Z'_{mn} standardizes the matrix for negative indicators.

(2) Determine the weight of indicators. The entropy weight method is a method that calculates the entropy value of each indicator based on its impact on the overall value and then determines the objective weight of the indicator by determining the weight [23,24]. The weight calculation method is shown in Equations (7)–(11).

$$P_{mn} = \frac{Z_{mn}}{\sum_{n=1}^{N} Z_{m,n}} \tag{7}$$

$$e_m = -C \times \sum_{n=1}^{N} (P_{mn} \times \ln(P_{mn})) \tag{8}$$

$$C = \ln(n) \tag{9}$$

$$d_m = 1 - e_m \tag{10}$$

$$w_m = \frac{d_m}{\sum_{m=1}^{M} d_m} \tag{11}$$

where P_{mn} indicates the nth sample value under the mth indicator, e_m is the information entropy for the mth indicator, d_m is the value of information utility, and w_m is the weight coefficient.

(3) Calculate the comprehensive score by constructing a weighted matrix using the TOPSIS method, which allows for an objective evaluation of each index while minimizing the influence of subjective factors. Based on the weighted matrix, select the positive and negative ideal solutions, and determine the distances from each operating condition to these ideal solutions. Use Formulas (12)–(17) to calculate the comprehensive score for each operating condition. A value closer to 1 indicates a better result, representing the optimal overall performance of the filter.

$$Z_m = w_m \times Z_{mn} \tag{12}$$

$$Z_m^+ = max(Z_m) \tag{13}$$

$$Z_m^- = min(Z_m) \tag{14}$$

$$D_n^+ = \sqrt{\sum_{m=1}^{M} \left(Z_m^+ - Z_m\right)^2} \tag{15}$$

$$D_n^- = \sqrt{\sum_{m=1}^{M} \left(Z_m^- - Z_m\right)^2} \tag{16}$$

$$R_n = \frac{D_n^-}{D_n^+ + D_n^-} \tag{17}$$

where D^+_n and D^-_n are the intercepts of positive and negative ideal solutions, respectively; Z^+_m and Z^-_m are the vectors of positive and negative ideal solutions, respectively; and R_n indicates the comprehensive score index of the nth option, $0 \leq R_n \leq 1$.

2.5. Data Statistical Analysis

The experimental results were plotted using Origin 2021 software, while statistical analysis was performed with SPSS 27.0. A one-way ANOVA was conducted, followed by LSD multiple comparisons for significance testing.

3. Results and Discussion

3.1. Changes in Head Loss of Drip Irrigation Filters with Clear Water

Figure 2 and Table 3 illustrate the changes in head loss across different types of filters under different flow conditions. As shown, there are significant differences in head loss value among the filter types, particularly between individual filters and combination filters, which display notably distinct variation patterns. In general, local head loss increases as system overcurrent rises. For a more precise analysis, the head loss of both single filters and combination filters at different flow rates were fitted according to Equation (1), resulting in the following Formulas: $h_j = kq^2$ for a single filter and $h_j = kq^{1.2}$ for a combination filter. The determination coefficients (R^2) for both equations exceed 0.96, indicating a strong correlation between the observed and predicted values. At a given flow rate, the head loss for high-mesh filters is consistently greater than that for low-mesh filters. In the case of combination filters, the total head loss at low flow rates ($q \leq 2.5$ m^3/h) is approximately equal to the sum of the head losses of the individual filters operating separately. However, at higher flow rates, the head loss of the combination filter is less than the sum of the individual filter losses, with the discrepancy increasing as the flow rate increases. Moreover, under identical conditions, the local head loss for disk filters is significantly higher than that for screen mesh filters. This difference grows as the flow rate increases. For instance, when the flow rate ranges from 1.5 to 3.5 m^3/h, the head loss difference between disk filters and screen mesh filters with the same mesh size increasing from 0.1 m to approximately

0.8 m. Finally, under consistent conditions, the order of stable local head loss values h_j for all filter treatments is as follows: S8 > S7 > S6 > S5 > S4 > S2 > S3 > S1.

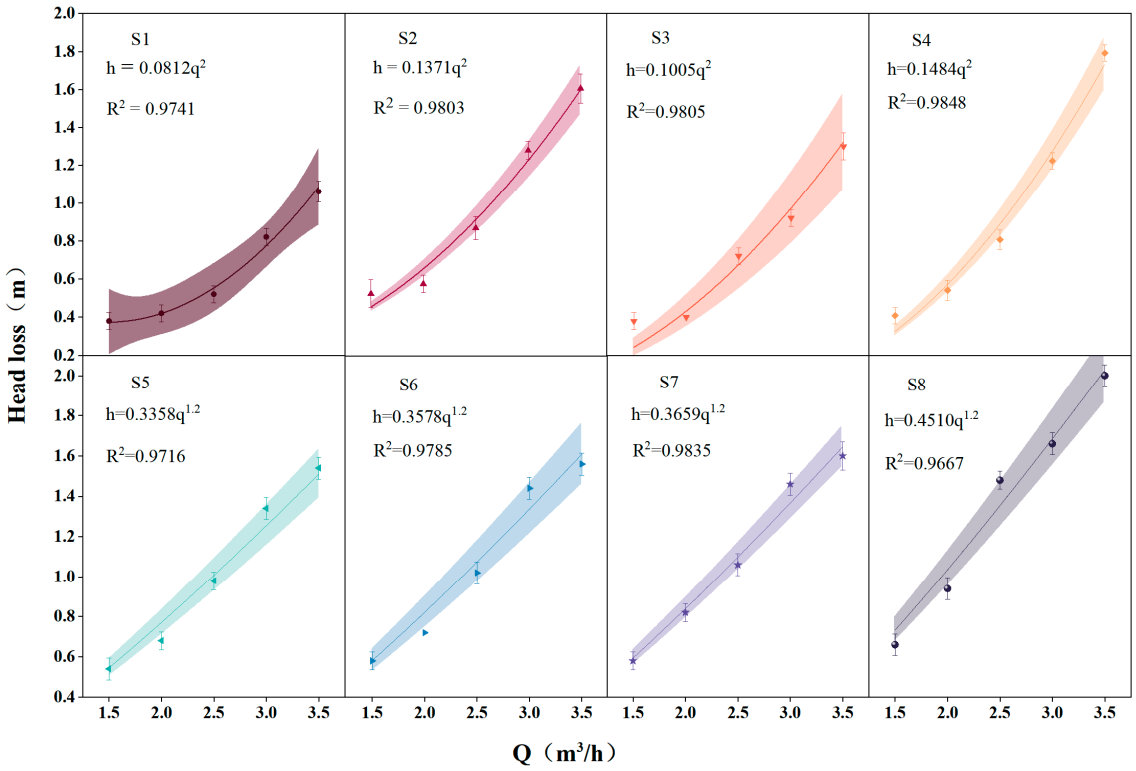


Figure 2. Effect of univariate cleaning on the hydraulic performance of the filter screen.

Table 3. The impact of flow rate changes on filter head loss.

Filter Type	S1	S2	S3	S4	S5	S6	S7	S8
1.5 m^3/h	0.38	0.38	0.38	0.42	0.54	0.58	0.58	0.66
2.0 m^3/h	0.42	0.44	0.4	0.56	0.68	0.72	0.82	0.94
2.5 m^3/h	0.52	0.78	0.72	0.84	0.98	1.02	1.06	1.48
3.0 m^3/h	0.82	1.26	0.92	1.28	1.34	1.44	1.46	1.66
3.5 m^3/h	1.06	1.64	1.3	1.88	1.54	1.56	1.6	2

In this study, all filters were housed in identical casings, so the differences in head loss coefficients k can be attributed solely to variations in the filter cartridges. As shown in Figure 2, the fitted formula for the disk filter has a larger coefficient k than the screen mesh filter. This is due to significant differences in the filter elements of the two types. In a screen mesh filter, the water flows through the mesh over a relatively short distance, resulting in two-dimensional filtration. In contrast, in disk filters, the water flows through the grooves of the filter over a longer distance, leading to three-dimensional filtration [25]. The relationship between head loss and flow rate in combination filters appears to be less pronounced, with the flow-rate to head-loss relationship index α being smaller than in single filters. This can be attributed to the complex flow dynamics inside the combination filters, particularly after a large-pore pre-filter (178–180 μm) is added to a small-pore (125 μm) screen mesh or disk filter. This configuration results in a head loss in the combination filter that is much smaller than the sum of the individual filter head losses, with the former being about 46% to 67% of the latter. This suggests that the head loss in combination filters cannot be calculated as a simple sum, but rather must be adjusted based on the flow rate [26].

3.2. Changes in Hydraulic Performance of Biogas Slurry Drip Irrigation Filter

3.2.1. Variation of Filter Head Loss with Respect to Different Flow Rates

Figure 3 illustrates the variation in head loss for each filter (and filter combination) under three different flow conditions, with a biogas slurry-to-water volume ratio of 1:14. As shown, the inflow rate significantly affects filter performance, particularly in terms of the rate of change in head loss. Based on these changes, the filter's operation can be divided into two distinct stages: the stable operation stage (t_1) and the clogged operation stage (t_2). In Figure 3, the stable operation stage (t_1) corresponds to the area to the left of the vertical dashed line, while the clogged operation stage (t_2) is represented to the right of the line. From the figure, it is evident that as the flow rate increases, the operating time for both stages becomes shorter. This leads to an increased rate of change in head loss. Additionally, the overall blockage uniformity (η) generally decreases with higher flow rates (Table 4). This finding is similar to the conclusion reached by Li et al. [19] in their study on sediment-laden water. For higher flow rates, the rate of change in head loss between the clogging and stable operation phases is lower, which aligns with the basic principles of fluid dynamics [27], which suggests that as the flow rate increases, the water speed through the filter medium also increases, resulting in a higher impurity load per unit of time. This reduces the operational duration of both filtration stages and accelerates the increase in head loss. For all filter combinations, the longest operating time occurs at a flow rate of Q = 1.5 m^3/h. Interestingly, some filters, such as S1 (80 mesh screen) and S3 (120 mesh), exhibit a longer stable operation time at Q = 3.5 m^3/h compared to Q = 2.5 m^3/h. This could be because, at higher flow rates, some suspended solids are pushed through the filter element, reducing clogging. However, this also diminishes the filter's ability to intercept impurities effectively Additionally, in the first stage (t_1), head loss fluctuates around a stable value, with this value increasing as the flow rate rises. At Q = 3.5 m^3/h, the stable head loss value reaches its highest point, approximately 2 m, which is significantly greater than the initial head loss. At Q = 1.5 m^3/h, the boundary between the two filtration stages is more clearly defined, and the blockage uniformity η peaks at around 1.75–11.38. At the other two flow rates, the boundary between the two stages is less distinct, and η shows little variation with increasing flow rates, lacking a clear trend.

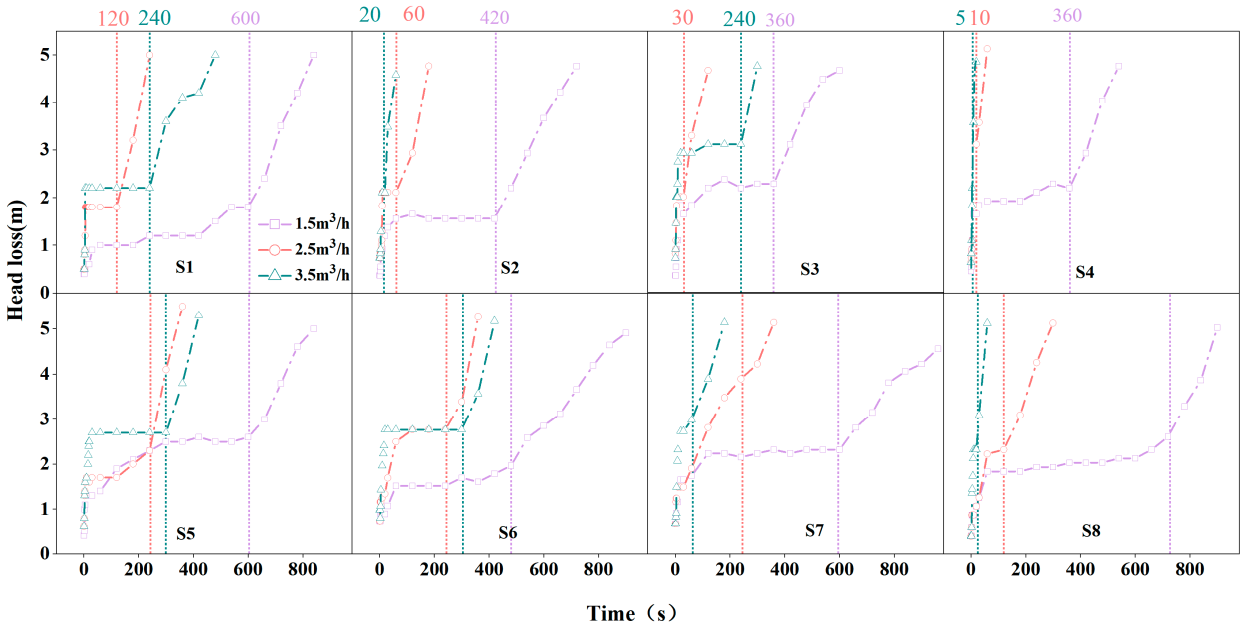


Figure 3. Changes in head loss of each filter under three different flow rates (biogas slurry:clean water 1:14).

Table 4. The performance indicators of the filter vary with concentration and flow rate.

FI SI/mm	Treatment	t_1/s	t_2/s	T	δ_1	δ_2	h_{j1}	h_{j2}	h_{j0}	η	DW
S1 0.180	Q1.5-C1:14	600	240	840	0.003	0.013	1.8	3.2	0.38	4.44	440.33
	Q2.5-C1:14	120	120	240	0.015	0.027	1.8	3.2	0.52	1.78	383.00
	Q3.5-C1:14	240	240	480	0.009	0.012	2.2	2.8	1.06	1.27	327.33
	Q2.5-C1:19	1560	540	2100	0.002	0.004	2.7	2.3	0.52	2.46	497.00
	Q2.5-C1:9	4	10	14	0.625	0.250	2.5	2.5	0.52	0.40	307.00
S2 0.180	Q1.5-C1:14	420	300	720	0.004	0.011	1.7	3.3	0.38	2.72	935.67
	Q2.5-C1:14	60	120	180	0.038	0.023	2.3	2.7	0.78	0.59	1060.67
	Q3.5-C1:14	20	40	60	0.115	0.068	2.3	2.7	1.64	0.59	1552.00
	Q2.5-C1:19	1260	600	1860	0.002	0.004	2.5	2.5	0.78	2.10	1315.67
	Q2.5-C1:9	6	7	13	0.233	0.514	1.4	3.6	0.78	2.20	909.67
S3 0.125	Q1.5-C1:14	240	60	300	0.008	0.050	2	3	0.38	6.00	208.67
	Q2.5-C1:14	30	90	120	0.073	0.031	2.2	2.8	0.72	0.42	167.00
	Q3.5-C1:14	360	240	600	0.006	0.012	2.2	2.8	1.3	1.91	124.00
	Q2.5-C1:19	780	660	1440	0.003	0.004	2.2	2.8	0.72	1.50	463.33
	Q2.5-C1:9	1	6	7	0.500	0.750	0.5	4.5	0.72	1.50	122.00
S4 0.125	Q1.5-C1:14	360	240	600	0.007	0.012	2.4	2.8	0.42	1.75	990.67
	Q2.5-C1:14	10	110	120	0.120	0.035	1.2	3.8	0.84	0.29	979.67
	Q3.5-C1:14	5	15	20	0.480	0.213	2.4	3.2	1.88	0.44	932.33
	Q2.5-C1:19	780	300	1080	0.003	0.008	2.5	2.5	0.84	2.60	1909.67
	Q2.5-C1:9	3	4	7	0.400	1.025	1.2	4.1	0.84	2.56	995.33
S5 0.18 & 0.125	Q1.5-C1:14	600	240	840	0.002	0.015	1.4	3.6	0.54	6.43	458.33
	Q2.5-C1:14	120	240	360	0.014	0.014	1.7	3.3	0.98	0.97	420.33
	Q3.5-C1:14	300	120	420	0.009	0.019	2.7	2.3	1.54	2.13	371.33
	Q2.5-C1:19	2460	120	2580	0.001	0.030	3.2	3.6	0.98	23.06	505.33
	Q2.5-C1:9	13	7	20	0.138	0.529	1.8	3.7	0.98	3.82	457.00
S6 0.18 & 0.126	Q1.5-C1:14	480	420	900	0.004	0.008	1.7	3.3	0.58	2.22	1579.33
	Q2.5-C1:14	240	120	360	0.006	0.030	1.4	3.6	1.02	5.14	1082.67
	Q3.5-C1:14	300	120	420	0.009	0.020	2.6	2.4	1.56	2.31	531.67
	Q2.5-C1:19	1500	1140	2640	0.001	0.004	1.3	4.1	1.02	4.15	1681.67
	Q2.5-C1:9	9	9	18	0.211	0.378	1.9	3.4	1.02	1.79	660.00
S7 0.18 & 0.127	Q1.5-C1:14	600	360	960	0.004	0.008	2.3	2.7	0.58	1.96	1624.67
	Q2.5-C1:14	60	300	360	0.030	0.011	1.8	3.2	1.06	0.36	1511.00
	Q3.5-C1:14	60	120	180	0.038	0.023	2.3	2.7	1.6	0.59	1282.00
	Q2.5-C1:19	1440	1080	2520	0.001	0.004	1.7	4	1.06	3.14	1719.00
	Q2.5-C1:9	4	8	12	0.150	0.588	0.6	4.7	1.06	3.92	1236.67
S8 0.18 & 0.128	Q1.5-C1:14	720	180	900	0.002	0.021	1.3	3.7	0.66	11.38	2626.00
	Q2.5-C1:14	30	270	300	0.043	0.014	1.3	3.7	1.48	0.32	2554.00
	Q3.5-C1:14	20	40	60	0.120	0.065	2.4	2.6	2	0.54	2537.00
	Q2.5-C1:19	1500	1080	2580	0.001	0.003	2.2	3.1	1.48	1.96	2650.67
	Q2.5-C1:9	3	6	9	0.200	0.750	0.6	4.5	1.48	3.75	2629.33

3.2.2. Changes in Head Loss Under Different Concentrations of Biogas Slurry

Figure 4 and Table 4 show the changes in head loss of each filter (or filter combination) under three different concentrations of biogas slurry at a flow rate of Q = 2.5 m^3/h. As depicted in Figure 4, there are notable differences in the variation of filtration head loss under different concentrations of biogas slurry. As the concentration increases, the rate of change in head loss also increases for all filters. Similar to the variation in head loss under different flow rates, the operation process is divided into two stages: the stable operation stage (t_1, left of the dashed line) and the blockage operation stage (t_2, right of the dashed line). Both the duration of the stable stage (t_1) and the blockage stage (t_2) decrease with increasing concentration, leading to a faster rate of head loss change.

The uniformity of filter blockage is generally lowest when the biogas slurry-to-water volume ratio is 1:14 across the three concentration levels. Both decreasing and increasing concentrations tend to increase filter blockage uniformity. Initially, the head loss before and after the filter increases sharply over time. After the inflection point, head loss stabilizes and accumulates until it reaches a critical blockage condition. This is due to the higher concentration of biogas slurry and impurities, which accelerates the blockage accumulation process on the filter medium, shortening the operating time and increasing the rate of head

loss change in both stages. Moreover, the rate of change in head loss during the blockage operation stage is faster than during the stable operation stage. This overlaps with the findings of Li et al. [19] regarding filter performance in high-sediment water. During the stable stage (t_1), head loss fluctuates around a certain stable value, with the stable value increasing as the concentration of biogas slurry rises. When the biogas slurry-to-water ratio is 1:9, this stable value is the highest, reaching about 2 m of head loss. At low concentrations, the boundary between the two filtration stages is distinct, whereas at higher concentrations, this boundary becomes less clear. These differences in head loss changes under varying inflow conditions confirm the findings of Liu et al. [28], particularly the significant increase in the rate of head loss change with variations in concentration.

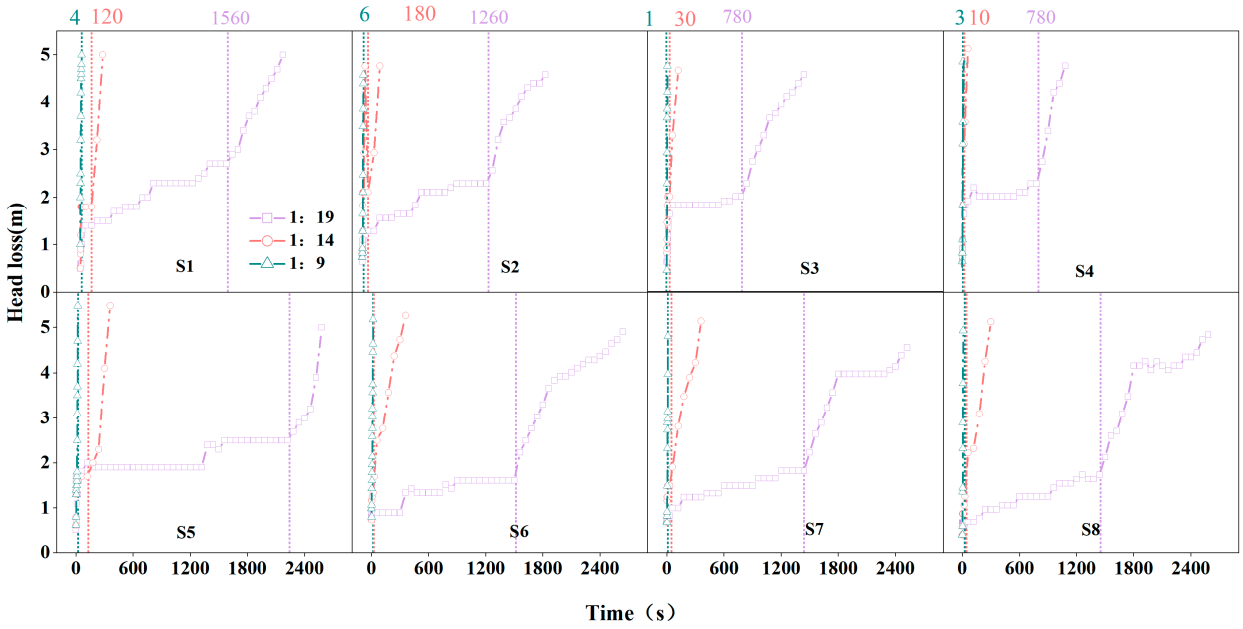


Figure 4. Changes in head loss of each filter under three different concentrations of biogas slurry (flow rate 2.5 m^3/h).

3.2.3. Changes in Head Loss of Different Filters and Their Combinations

By comparing Figures 3 and 4, it is evident that changes in inlet conditions affect each filter type and their combinations differently. For filters of the same type, small mesh filters exhibit lower initial head loss than large mesh filters, while large mesh filters show better filtration accuracy. The pattern of change in filter head loss is similar for both mesh and disk filters: as the flow rate or biogas slurry concentration increases, the rate of head loss increases sharply. This discovery is consistent with the research results of Tao et al. on micro irrigation filters [29], and the overall blockage uniformity decreases. However, disk filters experience a slower rate of change in head loss compared to mesh filters, and their blockage uniformity is lower, meaning the ratio of the blockage phase to the stable increase phase is smaller. This is corroborated by the experimental results of Li et al. [19]. Despite changes in inflow conditions, disk filters maintain stable performance, which aligns with the findings of Li et al. [30]. Compared to a single filter, a combination filter exhibits a smaller rate of change in head loss, lower blockage uniformity, and a more stable filtration process. Among the four filter combinations, the setup with a disk filter as the pre-filter and a mesh filter as the post-filter shows the smallest overall rate of change in head loss and the least blockage uniformity. In other words, this filter combination is less affected by changes in inlet conditions.

3.3. Variation Law of Total Operating Time of Biogas Slurry Drip Irrigation Filter

From Figure 5a,b, it can be seen that as the flow rate or concentration of the biogas slurry increases, the overall operating time of each filter and its combination gradually decreases. This is because increasing the flow rate or concentration will increase the amount of biogas slurry filtered per unit time, increase the risk of filter blockage, and thus shorten the filtration cycle. However, the flow rate has its own characteristics. When the increase exceeds a certain limit, the operating time will increase. This may be because when the flow rate is too high, some suspended solids will squeeze through the filter element with the high flow rate water flow, alleviating the filter blockage situation but at the same time reducing the interception effect of the filter. For example, some filters have a longer stable operating time at Q = 3.5 m^3/h compared to Q = 2.5 m^3/h, such as S1 (80 mesh), S3 (120 mesh), etc. Relative flow rate and operating time are greatly affected by concentration, and all filter combinations have the longest operating time when the volume ratio of biogas slurry to water is 1:19. At the same time, different types of filters also exhibit different operating time characteristics. Specifically, for all treatments at different flow rates and concentrations, mesh filters, due to their larger filtration area and relatively simple structure, usually provide longer operating time, while disk filters, although having high filtration capacity and self-cleaning characteristics, have relatively shorter operating time when treating water bodies with the same flow rate. The mesh size of the filter has a significant impact on the running time, and small mesh filters have a longer running time compared to large mesh filters. The performance differences between different types of filters under different inlet conditions, such as mesh filters running longer than disk filters, remain basically consistent. This further confirms the close relationship between filter performance and inlet conditions, including flow rate and concentration [31,32]. Among mesh filters, mesh filters have a longer filtration operation time compared to disk filters.

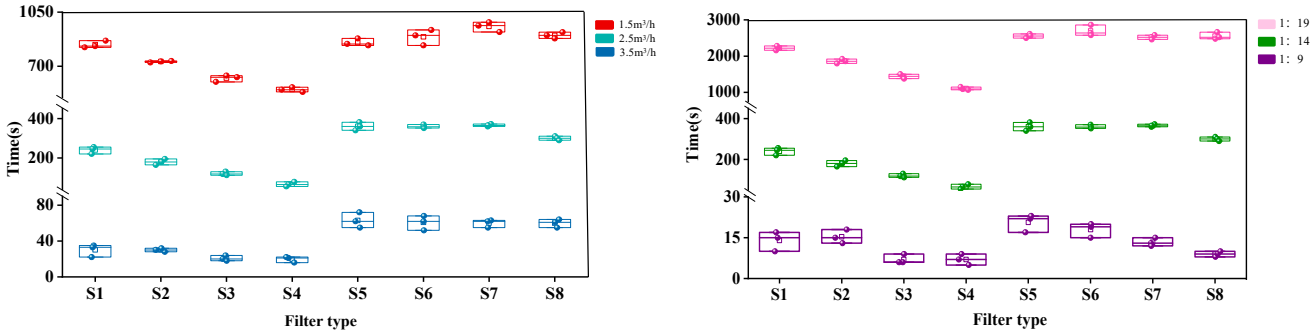


Figure 5. The variation pattern of running time of each filter. (**a**) The variation law of operating time of each filter under three different flow rates and (**b**) the variation law of operating time of each filter combination under three different concentrations.

At all flow rates and concentrations, the anti-clogging performance of the four combined filters is superior to that of the four single filters, manifested in the longer operating cycle of the combined filters compared to the single filters. In terms of running time, the combination filter is about 88~167% of the pre-filter and about 130~300% of the post-filter. The combination filter achieves complementary and optimized performance by connecting different types or mesh filters in series. For the combination filter, the larger pore size of the pre-filter also means that large particle impurities can be quickly removed in the early stage of filtration, delaying the clogging process of the filter medium and prolonging the operation time of the combination filter. This result verifies the experimental conclusion of Tian et al. [33]. There is no significant difference in the operating cycle of four different

filter combinations under the working conditions of equal flow rate and concentration of biogas slurry water. Compared to a single 80 mesh filter, the combined filter has undergone secondary filtration of the biogas slurry, achieving the requirement of 120 mesh filtration and high filtration accuracy. In addition, the running time of the combination filter is basically determined by the running time of its pre-filter. This is because the pre-filter, as the first line of defense, undertakes the main task of removing large particle impurities, thereby reducing the burden on subsequent filtering units. At the same time, the combination filter inherits the long operating cycle of small mesh filters and further improves the filtration accuracy, meeting the high water quality requirements of micro irrigation systems. This design not only extends the overall service life of the filter but also effectively reduces the risk of system end blockage, improving the stability and reliability of the irrigation system.

3.4. Variation Law of Pollutant Holding Capacity of Filter Element

3.4.1. Influence of Flow Rate on the Pollutant Holding Capacity of Filter Cartridges

The variation law of the pollutant carrying capacity of each filter element at different flow rates is shown in Figure 6. The experimental results demonstrate significant differences in pollutant carrying capacity among different types of filters. The pollutant holding capacity of disk filters is significantly better than that of mesh filters, about three times that of the latter. This discovery is of great significance for the design and optimization of practical water treatment systems, as disk filters can more effectively remove suspended solids under the same conditions, reduce the frequency of filter element replacement, and thus lower maintenance costs. The combination of mesh filters did not significantly improve its pollutant holding capacity and performed similarly to a single 80 mesh screen mesh filter. However, the combination of pure disk filters exhibits a stronger pollutant holding capacity, almost equal to the sum of the effects of two separate disk filters. This indicates that disk filters can exert a synergistic effect when used in combination, enhancing the overall filtering effect [34]. This discovery provides an important basis for filter combination design, especially in situations where high pollutant holding capacity is required. The relationship between the pollutant holding capacity and flow rate of different types of filters is complex and diverse. The fouling capacity of the screen mesh filter element is negatively correlated with the flow rate, which may be due to the fact that the smaller the flow rate, the easier it is to slowly form a filter cake layer on the surface of the mesh, thereby accelerating the sedimentation rate of subsequent suspended solids [35]. On the contrary, the fouling capacity of the 80 mesh disk filter cartridge is positively correlated with the flow rate, which may be related to the larger pore size of the disk filter and the easier deposition of blockages when the flow rate increases. However, the 120 mesh disk filter and disk combination filter showed no significant negative correlation, which may be due to their small pores and easy blockage of large suspended particles, resulting in an insignificant impact of flow rate changes on the total amount of blockage accumulation. Compared to a single filter, a combination filter of the same type exhibits smaller fluctuations in flow rate, indicating that the combination filter has higher stability in dealing with flow rate changes. This characteristic is particularly important in practical applications, as water treatment systems often face flow fluctuations. Combination filters can provide more stable filtering effects and reduce the decline in filtering performance caused by flow changes, thereby extending the service life of equipment and reducing maintenance costs.

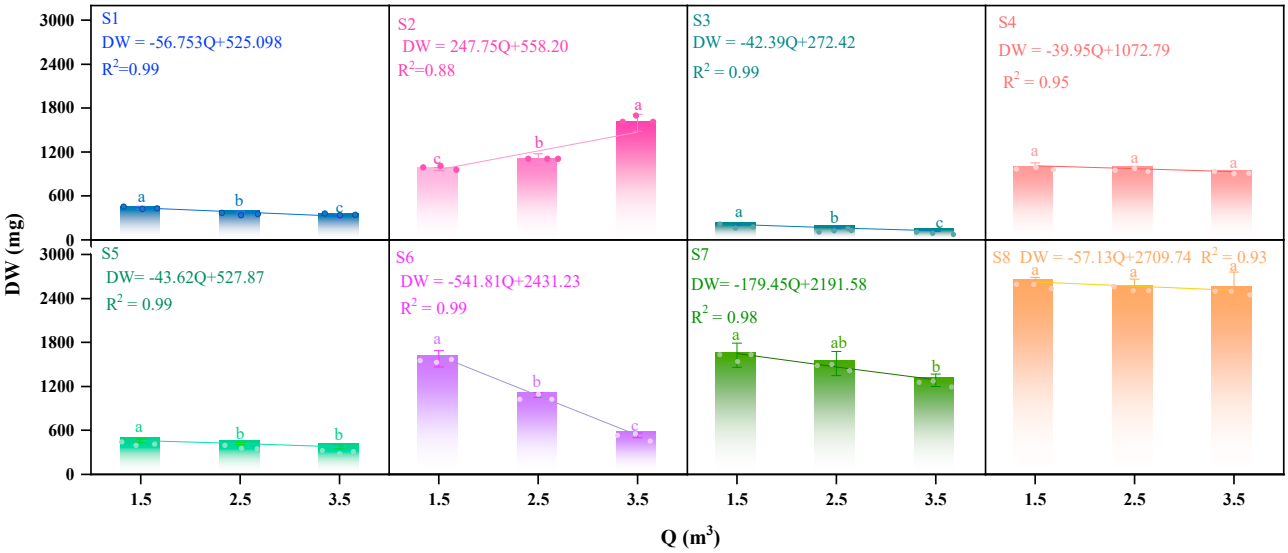


Figure 6. The variation law of pollutant carrying capacity of each filter element at different flow rates (volume ratio of biogas slurry to water 1:14). Different letters represent different treatments with significant differences under $p < 0.05$.

3.4.2. Influence of Biogas Slurry Concentration on the Pollutant Carrying Capacity of Filter Cartridges

The variation pattern of the pollutant carrying capacity of all filter cartridges under different concentrations of biogas slurry is shown in Figure 7. The significance labeling of the variance analysis of DW with changes in biogas slurry concentration in Figure 7 indicates that when the volume ratio of biogas slurry to water is between 1:14 and 1:9, there is no significant positive correlation between the concentration of biogas slurry and the capacity of the filter cartridge in combination filters S7 and S8. As the biogas slurry concentration increases, the contaminant load on the filter cartridge increases by 13.77% and 3.57%, respectively. This may indicate that these two combination filters are less sensitive to fouling at lower to medium concentrations or that their combination structure helps to slow down the fouling rate at lower to medium concentrations. The other six treatments showed a significant positive correlation. As the biogas slurry concentration increases, the contaminant load on the filter cartridge increases by 20.22% to 177.44%, respectively, indicating that the fouling capacity of these filters significantly increased with the increase of biogas slurry concentration. This means that these filters require more frequent cleaning or replacement of the filter cartridges at higher concentrations. When the volume ratio of biogas slurry to water is between 1:19 and 1:14, the fouling capacity of filters S1 and S6 is significantly positively correlated with the concentration of biogas slurry. The contaminant load on the filter cartridge increases by 24.76% and 63.87%, respectively, as the concentration increases, indicating that these filters are more sensitive to fouling at higher concentrations. Filters S4, S5, and S8 show no significant negative correlation. As the concentration increases, it decreases by 1.57%, 8.02%, and 2.66%, respectively, which may be due to the specific flow conditions or filter material characteristics of these filters within this concentration range, and further research is needed to understand their specific mechanisms. The remaining three treatments show an insignificant positive correlation, indicating that as the DW increases at medium and low concentrations, the significance between the groups is all less than 0.05. This suggests that in the medium and low concentration range, as the concentration increases, the contaminant loading rate of these three filter groups does not significantly accelerate.

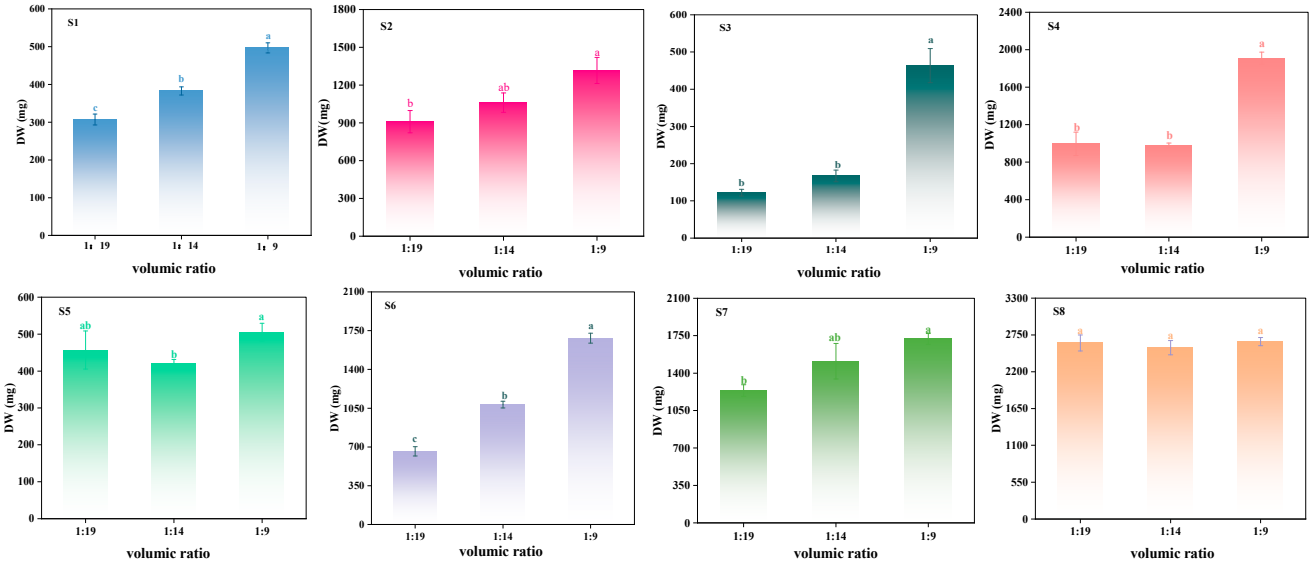


Figure 7. The variation pattern of pollutant carrying capacity of each filter element under different concentrations of biogas slurry (flow rate 2.5 m^3/h), Different letters represent different treatments with significant differences under $p < 0.05$.

Filters of the same type exhibit different patterns of pollutant absorption under different concentrations of biogas slurry. For screen mesh filters, there is no significant difference in the pollutant carrying capacity of each filter at high concentrations (1:9), which may be due to the common influence of the complex components of high-concentration biogas slurry on the pollutant carrying capacity of the filter element masking the differences in mesh size or combination methods. For filters of the same type, the difference in contaminant load at medium and low concentrations (1:19 and 1:14) is not significant (S1, S4, and S8). The combination filter has the highest contaminant load, approximately twice that of a single filter, followed by the 80 screen mesh filter and the 120 mesh screen mesh filter having the smallest. This may indicate that at high concentrations, the influence of physical structure differences on pollutant absorption is weakened, while at low concentrations, the fineness of the filter becomes a key factor. There is a significant difference in the fouling capacity of disk filters at any concentration, and the combined filter has the highest fouling capacity, followed by 120 mesh and finally 80 mesh. This reflects the significant impact of the special structure and filtering mechanism of disk filters on the pollutant holding capacity under different mesh sizes and combinations. Under different concentrations of biogas slurry, the fouling capacity of laminated filters is much higher than that of mesh filters for different types of filters. This may be due to the structural characteristics of laminated filters, which make them easier to capture and accumulate impurities in biogas slurry. In the combination filter, the type of pre-filter has a significant impact on the pollutant holding capacity. At high concentrations, the effect of pre-filter type on the combined pollutant holding capacity is not significant; however, at low to medium concentrations, the combination of disk filters as a pre-filter has a significantly higher pollutant absorption capacity than mesh filters, which may indicate that disk filters are more likely to capture small particles [36], thereby accelerating the pollutant absorption of subsequent filter layers.

Based on the above results and analysis, it is recommended to prioritize the use of disk filters and their combination forms in situations where high pollutant absorption capacity and stable filtration efficiency are required. At the same time, when designing filter systems, the impact of flow rate changes and wastewater loading on filtration performance should be fully considered [37,38], and suitable combination methods and filter types should be

selected to cope with different application scenarios. In addition, regular monitoring and maintenance of filters are also key measures to ensure their long-term stable operation [39].

3.5. Comprehensive Evaluation and Optimization of Filters for Biogas Slurry Drip Irrigation System

The entropy weight TOPSIS comprehensive evaluation method was used to evaluate the changes in filter head loss while considering the pollutant carrying capacity DW and filtration accuracy. The weights of each evaluation index were calculated and shown in Table 5. The weight of the filter running time T is the highest, at 46%, followed by the pollutant carrying capacity DW and filtration accuracy, at 23.62% and 20.61%, respectively. In the comprehensive evaluation, T represents hydraulic performance, DW represents pollutant carrying performance, and M filtration accuracy performance, all of which are positive indicators. The weights of the negative indicators, η and h_j, are relatively low. Among them, η represents the ratio of the growth rate of the head loss in the second stage to that in the first stage. The smaller the η, the more stable the filter performance and the better the operating effect. h_j represents the initial head loss of the filter. The smaller the initial head loss, the better the hydraulic performance of the filter. In summary, positive indicators have the main impact on the comprehensive performance evaluation of filters, accounting for about 90% of the weight, while negative indicators have a minor impact on the comprehensive performance evaluation of filters, accounting for only 10% of the weight.

Table 5. Weight of each evaluation index.

Evaluation Index	Weight/%
Total operation time (T)	46.00
dry weight of pollutant carrying capacity (DW)	23.62
Filter mesh size (M)	20.61
Clogging uniformity (η)	2.23
Initial head loss (h_j)	7.54

Substituting the weights of each indicator into TOPSIS, Table 6 shows the comprehensive evaluation results of TOPSIS. The top three are the filter combinations S8, S6, and S7 under the conditions of Q = 2.5 m^3/h and 1:19 volume of biogas slurry and water. The comprehensive results are 0.994, 0.985, and 0.982, respectively. For low biogas slurry concentration, under the three flow conditions, all treatments were ranked higher in terms of comprehensive ranking, with smaller h_j and η and longer T. Among them, the fouling capacity of the disk filter was greater than that of the screen mesh filter. When the disk filter was used as a pre-filter, the hydraulic performance of the filter combination was better. For the concentration of high biogas slurry, the comprehensive performance of the combined filter is better than that of a single filter. This is because the operating time T and pollutant holding capacity DW of the combined filter are slightly higher than those of a single filter, and the filtration accuracy (M) is higher than that of two small mesh filters. The initial head loss is lower than that of a single filter, and the η of the combined filter is also lower than that of a single filter. This is because the initial head loss h_j of the combination filter and the two filters are measured separately, and the pre-filter and post-filter, respectively, intercept a part of the dirt, effectively reducing the initial head loss and the rate of change in head loss, making the filtration more stable.

Overall, Q = 2.5 m^3/h and the ratio of slurry-to-water volume of 1:19 are more conducive to the stability and long-term operation of the filter. The combined filter has better comprehensive performance. Compared with the screen mesh filter, the disk filter has better comprehensive performance as a pre-filter. When the screen mesh filter and disk filter are used as post-filters, their comprehensive performance is not significantly different, each with its own advantages and disadvantages. The initial head loss of the

screen mesh filter is smaller, and the fouling capacity of the disk filter is larger. In this study, the TOPSIS entropy weight method model is used to quantify and assign weights to various filter indicators. Based on the assigned weights, filters are scored under different inlet conditions, providing a straightforward and effective way to select filters. However, for the TOPSIS-entropy weight evaluation, this is a new method that requires further validation in other areas to improve its effectiveness [40].

Table 6. Entropy weight-TOPSIS comprehensive analysis of hydraulic performance of various filters under different operating conditions.

Treatment	Scoring Index	Sorting Results	Treatment	Scoring Index	Sorting Results
S1-Q1.5-C1:14	0.468	31	S5-Q1.5-C1:14	0.652	12
S1-Q2.5-C1:14	0.226	39	S5-Q2.5-C1:14	0.521	23
S1-Q3.5-C1:14	0.288	37	S5-Q3.5-C1:14	0.538	21
S1-Q2.5-C1:19	0.801	7	S5-Q2.5-C1:19	0.925	4
S1-Q2.5-C1:9	0.174	40	S5-Q2.5-C1:9	0.466	32
S2-Q1.5-C1:14	0.469	30	S6-Q1.5-C1:14	0.744	11
S2--Q2.5-C1:14	0.298	36	S6-Q2.5-C1:14	0.575	18
S2-Q3.5-C1:14	0.344	35	S6-Q3.5-C1:14	0.549	20
S2-Q2.5-C1:19	0.817	5	S6-Q2.5-C1:19	0.985	2
S2-Q2.5-C1:9	0.242	38	S6-Q2.5-C1:9	0.474	29
S3-Q1.5-C1:14	0.503	26	S7-Q1.5-C1:14	0.761	10
S3-Q2.5-C1:14	0.463	33	S7-Q2.5-C1:14	0.598	15
S3-Q3.5-C1:14	0.558	19	S7-Q3.5-C1:14	0.536	22
S3-Q2.5-C1:19	0.793	8	S7-Q2.5-C1:19	0.982	3
S3-Q2.5-C1:9	0.443	34	S7-Q2.5-C1:9	0.505	25
S4-Q1.5-C1:14	0.626	14	S8-Q1.5-C1:14	0.791	9
S4-Q2.5-C1:14	0.509	24	S8-Q2.5-C1:14	0.647	13
S4-Q3.5-C1:14	0.479	28	S8-Q3.5-C1:14	0.595	16
S4-Q2.5-C1:19	0.804	6	S8-Q2.5-C1:19	0.994	1
S4-Q2.5-C1:9	0.49	27	S8-Q2.5-C1:9	0.594	17

4. Conclusions

In this study, the comprehensive performance evaluation of two common types of filters and their combination filters was conducted based on indicators such as head loss, pollutant carrying capacity, and filtration accuracy. The entropy weighting method was used to assign weights, and the evaluation was performed under varying flow rates and concentrations in biogas slurry systems. The main conclusions are as follows:

(1) After testing common filters in the application of biogas slurry drip irrigation, it was found that the flow rate, concentration, and filter type in biogas slurry systems all significantly influence the hydraulic performance of the filter. Among these factors, concentration has a notably greater impact on the fouling capacity of the filter element than the flow rate. Medium to low concentrations are more conducive to the long-term operation of the filter. Small mesh filters exhibit lower initial head loss and longer operational lifetimes, but they have reduced filtration accuracy. In contrast, disk filters offer a higher pollutant holding capacity than screen mesh filters, with the pollutant retention of disk filters being approximately three times greater than that of screen mesh filters.

(2) A comprehensive performance evaluation model for filters was established. In the entropy weight-TOPSIS comprehensive evaluation, the running time and pollutant holding capacity of the filter are key factors affecting the overall performance of the filter. The running time, pollutant capacity, and filtration accuracy are positive indicators that have a major impact on the comprehensive performance evaluation of the filter, accounting for about 90% of the weight. The blockage uniformity and initial water loss are negative indicators that have a minor impact on the comprehensive performance evaluation of the filter, accounting for only 10% of the weight.

(3) The combination filter improves both the hydraulic performance and contaminant absorption capacity of the filter. Under all flow rates and concentrations, the hydraulic and contaminant removal performance of the four combination filters is superior to that of the four single filters. This is reflected in the longer operational cycles of the combination filters, which are approximately one to two times longer than those of the single filters. In terms of contaminant load, the combination filters typically have around twice the contaminant removal capacity of the single filters. Among them, when the disk filter is used as the pre-filter and the mesh filter as the post-filter in combination, the rate of head loss change is the smallest, and the clogging uniformity is the least. From the perspective of improving the operational stability of the slurry drip irrigation system, it is recommended to adopt a combination filtration method of disk + screen mesh.

In addition, compared to a single filter, although the combination filtering method extends the working time and improves the filtering accuracy, it compensates for the shortcomings of a single filter. However, in the biogas slurry drip irrigation system, regardless of the combination of filters, they tend to clog quickly. Therefore, frequent flushing is required. It is recommended to configure screen mesh or disk filters with automatic back-washing function.

Author Contributions: S.W. (Shuaijie Wang): Investigation, formal analysis, data curation, writing—original draft, writing—review & editing. H.W. (Haitao Wang): Investigation, formal analysis, writing—review, editing, funding acquisition. X.Q.: Investigation, formal analysis. J.W.: Conceptualization, writing—review & editing, funding acquisition. S.W. (Shuji Wang): Investigation, funding acquisition. H.W. (Hang Wang): Investigation, formal analysis. T.S.: Conceptualization, investigation. All authors have read and agreed to the published version of the manuscript.

Funding: This work was supported by the Changji Technology Innovation Team project (2023CT08), Bingtuan Science and Technology Program (2023AB071), and the Natural Science Foundation of Hebei Province (E2024402034), Xinjiang Uygur Autonomous Region "Tianchi Talents" introduction plan.

Institutional Review Board Statement: Not applicable.

Data Availability Statement: The raw data supporting the conclusions of this article will be made available by the authors upon request.

Conflicts of Interest: The authors declare that there are no conflicts of interest.

References

1. Jiang, Y.; Zhang, Y.; Li, H. Research Progress and Analysis on Comprehensive Utilization of Livestock and Poultry Biogas Slurry as Agricultural Resources. *Agriculture* **2023**, *13*, 2216. [CrossRef]
2. Tao, J.; Li, J.; Yan, B.; Chen, G.; Cheng, Z.; Li, W.; Lin, F.; Hou, L. Catalytic Reforming: A Potentially Promising Method for Treating and Utilizing Wastewater from Biogas Plants. *Environ. Sci. Technol.* **2020**, *54*, 577–585. [CrossRef]
3. Wang, H.; Wang, J.; Wang, C.; Wang, S.; Qiu, X.; Li, G. Adaptability of biogas slurry–water ratio and emitter types in biogas slurry drip irrigation system. *Agric. Water Manag.* **2022**, *274*, 107988. [CrossRef]
4. Li, J.; Yang, W.; Liu, L.; Liu, X.; Qiu, F.; Ma, X. Development and environmental impacts of China's livestock and poultry breeding. *J. Clean. Prod.* **2022**, *371*, 133586. [CrossRef]
5. Zeng, W.; Qiu, J.; Wang, D.; Wu, Z.; He, L. Ultrafiltration concentrated biogas slurry can reduce the organic pollution of groundwater in fertigation. *Sci. Total Environ.* **2022**, *810*, 151294. [CrossRef]
6. Hu, B.; Jiang, M.; Zhao, S.; Ji, X.; Shu, Q.; Tian, B.; He, T.; Zhang, L. Biogas slurry as draw solution of forward osmosis process to extract clean water from micro-polluted water for hydroponic cultivation. *J. Membr. Sci.* **2019**, *576*, 88–95. [CrossRef]
7. Wang, H.; Qiu, X.; Liang, X.; Wang, H.; Wang, J. Biogas slurry change the transport and distribution of soil water under drip irrigation. *Agric. Water Manag.* **2024**, *294*, 108719. [CrossRef]
8. Wang, H.; Wang, J.; Wang, C.; Wang, S.; Qiu, X.; Sun, Y.; Li, G. Characterization of labyrinth emitter-clogging substances in biogas slurry drip irrigation systems. *Sci. Total Environ.* **2022**, *820*, 153315. [CrossRef]

9. Li, Y.; Xu, S.; Zhao, M.; Song, Y.; Wang, Z.; Xie, X. Filtration with cornstalks as a pre-treatment process to control membrane fouling in the concentration of biogas slurry: Performance, mechanism and economic analysis. *Environ. Sci. Water Res. Technol.* **2022**, *8*, 1011–1020. [CrossRef]
10. Blume, T.; Neis, U. Improved wastewater disinfection by ultrasonic pre-treatment. *Ultrason. Sonochemistry* **2004**, *11*, 333–336. [CrossRef]
11. Alfonso-Muniozguren, P.; Serna-Galvis, E.A.; Bussemaker, M.; Torres-Palma, R.A.; Lee, J. A review on pharmaceuticals removal from waters by single and combined biological, membrane filtration and ultrasound systems. *Ultrason. Sonochemistry* **2021**, *76*, 105656. [CrossRef] [PubMed]
12. Badawi, A.K.; Kriaa, K.; Osman, R.M.; Hassan, R. Modified Rice Husk Waste-Based Filter for Wastewater Treatment: Pilot Study and Reuse Potential. *Chem. Eng. Technol.* **2024**, *47*, 968–975. [CrossRef]
13. Wang, H.; Zhao, H.; Wang, K.; He, Y.; Zheng, C. Simulation of filtration process for multi-fiber filter using the Lattice-Boltzmann two-phase flow model. *J. Aerosol Sci.* **2013**, *66*, 164–178. [CrossRef]
14. Heistad, A.; Paruch, A.M.; Vråle, L.; Ádám, K.; Jenssen, P.D. A high–performance compact filter system treating domestic wastewater. *Ecol. Eng.* **2006**, *28*, 374–379. [CrossRef]
15. Ma, X.Y.D.; Zeng, Z.; Wang, Z.; Xu, L.; Zhang, Y.; Ang, J.M.; Wan, M.P.; Ng, B.F.; Lu, X. Robust microhoneycomb-like nanofibrous aerogels derived from cellulose and lignin as highly efficient, low-resistant and anti-clogging air filters. *J. Membr. Sci.* **2022**, *642*, 119977. [CrossRef]
16. Liang, X.; Wang, C.; Wang, H.; Yao, Z.; Qiu, X.; Wang, J.; He, W. Biogas slurry topdressing as replacement of chemical fertilizers reduces leaf senescence of maize by up-regulating tolerance mechanisms. *J. Environ. Manag.* **2023**, *344*, 118433. [CrossRef] [PubMed]
17. Capra, A.; Scicolone, B. Assessing dripper clogging and filtering performance using municipal wastewater. *Irrig. Drain.* **2005**, *54*, S71–S79. [CrossRef]
18. Madeira, A.A. Major and minor head losses in a hydraulic flow circuit: Experimental measurements and a Moody's diagram application. *Eclética Química* **2020**, *45*, 47–56. [CrossRef]
19. Li, L.; Zhu, D.; Zhang, R.; Zheng, C.; Zhao, Z.; Hong, M.; Khudayberdi, N.; Liu, C. Enhanced experimental study on the head loss and filtration performance of annular flow disc filter. *Nygcxb* **2024**, *40*, 140–148. [CrossRef]
20. Li, W.; O'Kelly, B.C.; Fang, K.; Yang, M. Briefing: Water content determinations of peaty soils using the oven-drying method. *Environ. Geotech.* **2022**, *9*, 3–11. [CrossRef]
21. Bhadra, D.; Dhar, N.R.; Salam, M.A. Sensitivity analysis of the integrated AHP-TOPSIS and CRITIC-TOPSIS method for selection of the natural fiber. *Mater. Today Proc.* **2022**, *56*, 2618–2629. [CrossRef]
22. Wu, H.-W.; Li, E.; Sun, Y.; Dong, B. Research on the operation safety evaluation of urban rail stations based on the improved TOPSIS method and entropy weight method. *J. Rail Transp. Plan. Manag.* **2021**, *20*, 100262. [CrossRef]
23. Li, X.; Wang, K.; Liu, L.; Xin, J.; Yang, H.; Gao, C. Application of the Entropy Weight and TOPSIS Method in Safety Evaluation of Coal Mines. *Procedia Eng.* **2011**, *26*, 2085–2091. [CrossRef]
24. Chen, P. Effects of the entropy weight on TOPSIS. *Expert. Syst. Appl.* **2021**, *168*, 114186. [CrossRef]
25. Simon, M.; Vianello, A.; Vollertsen, J. Removal of >10 µm Microplastic Particles from Treated Wastewater by a Disc Filter. *Water* **2019**, *11*, 1935. [CrossRef]
26. Alazba, A.A.; Mattar, M.A.; ElNesr, M.N.; Amin, M.T. Field Assessment of Friction Head Loss and Friction Correction Factor Equations. *J. Irrig. Drain. Eng.* **2012**, *138*, 166–176. [CrossRef]
27. Jeon, S.; Heinz, U. Introduction to hydrodynamics. *Int. J. Mod. Phys. E* **2015**, *24*, 1530010. [CrossRef]
28. Liu, Z.; Lei, C.; Li, J.; Long, Y.; Lu, C. A Standardized Treatment Model for Head Loss of Farmland Filters Based on Interaction Factors. *Agriculture* **2024**, *14*, 788. [CrossRef]
29. Tao, H.; Shen, P.; Li, Q.; Jiang, Y.; Yang, W.; Wei, J. Research on head loss of pre-pump micro-pressure filter under clean water conditions. *Water Supply* **2021**, *22*, 3271–3282. [CrossRef]
30. Li, X.; Huang, G.; Li, Y.; Chen, X.; Yao, Y.; Liang, Y.; Huang, J.; Zhao, K.; Yin, J. Low-Cost ceramic disk filters coated with Graphitic carbon nitride (g-C_3N_4) for drinking water disinfection and purification. *Sep. Purif. Technol.* **2022**, *292*, 120999. [CrossRef]
31. Lin, W.; Lei, J.; Wang, Q.; Wang, X.; Huang, X. Performance enhancement of spiral-wound reverse osmosis membrane elements with novel diagonal-flow feed channels. *Desalination* **2022**, *523*, 115447. [CrossRef]
32. Xiong, Z.-C.; Zhu, Y.-J.; Wang, Z.-Y.; Chen, Y.-Q.; Yu, H.-P. Tree-Inspired Ultralong Hydroxyapatite Nanowires-Based Multifunctional Aerogel with Vertically Aligned Channels for Continuous Flow Catalysis. Water Disinfection, and Solar Energy-Driven Water Purification. *Adv. Funct. Mater.* **2022**, *32*, 2106978. [CrossRef]
33. Tian, X.; Ou, Q.; Liu, J.; Liang, Y.; Pui, D.Y.H. Influence of pre-stage filter selection and face velocity on the loading characteristics of a two-stage filtration system. *Sep. Purif. Technol.* **2019**, *224*, 227–236. [CrossRef]
34. Xu, X.; Wang, Q.; Zhang, J.; Zong, R.; Liu, N. Experimental Study of Filtration Performance of Disc Filter with Discrete Channel Structure. *J. Irrig. Drain. Eng.* **2023**, *149*, 7. [CrossRef]

35. Wakeman, R. The influence of particle properties on filtration. *Sep. Purif. Technol.* **2007**, *58*, 234–241. [CrossRef]
36. Duran-Ros, M.; Puig-Bargués, J.; Arbat, G.; Barragán, J.; de Cartagena, F.R. Performance and backwashing efficiency of disc and screen filters in microirrigation systems. *Biosyst. Eng.* **2009**, *103*, 35–42. [CrossRef]
37. Wilson, J.; Boutilier, L.; Jamieson, R.; Havard, P.; Lake, C. Effects of Hydraulic Loading Rate and Filter Length on the Performance of Lateral Flow Sand Filters for On-Site Wastewater Treatment. *J. Hydrol. Eng.* **2011**, *16*, 639–649. [CrossRef]
38. Li, N.; Li, J.; Yu, L.; Yang, W.; Liu, X.; Cheng, Q. Effect of inlet velocity on the hydraulic and filtering performance of a Y-type screen filter. *Irrig. Drain.* **2024**, *73*, 799–812. [CrossRef]
39. Coelho, R.D.; de Almeida, A.N.; Costa, J.d.O.; Pereira, D.J.d.S. Mobile drip irrigation (MDI): Clogging of high flow emitters caused by dragging of driplines on the ground and by solid particles in the irrigation water. *Agric. Water Manag.* **2022**, *263*, 107454. [CrossRef]
40. Delgado, A.; Romero, I. Environmental conflict analysis using an integrated grey clustering and entropy-weight method: A case study of a mining project in Peru. *Environ. Model. Softw.* **2016**, *77*, 108–121. [CrossRef]

Disclaimer/Publisher's Note: The statements, opinions and data contained in all publications are solely those of the individual author(s) and contributor(s) and not of MDPI and/or the editor(s). MDPI and/or the editor(s) disclaim responsibility for any injury to people or property resulting from any ideas, methods, instructions or products referred to in the content.